CYCLOTRON LINE FEATURES OF MAGNETIZED ACCRETING NEUTRON STARS

G. Schönherr[1,2,4], J. Wilms[2,3], P. Kretschmar[4], I. Kreykenbohm[1,5], A. Santangelo[1], R.E. Rothschild[6], and W. Coburn[7]

[1]*Institut für Astronomie und Astrophysik Tübingen, Sand 1, 72076 Tübingen, Germany*
[2]*Department of Physics, University of Warwick, Coventry, CV4 7AL, UK*
[3]*Dr. Remeis Sternwarte, FAU Erlangen-Nürnberg, Sternwartstr. 7, 96049 Bamberg, Germany*
[4]*European Space Astronomy Centre, ESA, Apartado 50727, 28080 Madrid, Spain*
[5]*INTEGRAL Science Data Centre, 16 Chemin d'Ecogia, 1290 Versoix, Switzerland*
[6]*CASS, University of California, San Diego, CA 92093-0111, USA*
[7]*SSL, University of California, Berkeley, CA 94720-7450, USA*

ABSTRACT

Providing the only known direct estimate of the magnetic field strength of an accreting neutron star, the study of 'Cyclotron Resonance Scattering Features' (often abbreviated CRSFs or cyclotron lines) is fundamental to a better understanding of the physics of those powerful X-ray sources. During the last three decades cyclotron lines have been detected as absorption features in many accreting neutron star binaries [1, 2, 3, 4]. The excellent energy resolution of todays' instruments on satellites such as *INTEGRAL* allows not only for the detection of cyclotron lines but also for a good resolution of their complex line shapes. Using a revised version of the Monte Carlo code by R. Araya [5, 6], we set up a preliminary model for cyclotron line formation and compare its predictions to observational data.

Key words: X-rays: stars; stars: neutron; magnetic fields; line: formation.

1. INTRODUCTION

Cyclotron lines have been observed as absorption features in the high-energy spectra of more than a dozen magnetized accreting neutron stars. They are indicators for the strong magnetic field of those neutron stars which quantizes the momenta of the electrons in the line-forming region in discrete Landau levels perpendicular to the field. Photons with energies of ($\sim n$ times) the fundamental Landau energy undergo resonant scattering with the electrons and are trapped in the dense plasma of the accretion mound. The observed spectrum thus exhibits absorption features at the line energies:

$$E_n = m_\mathrm{e}c^2 \frac{\sqrt{1+2nB/B_\mathrm{crit}\sin^2\theta}-1}{\sin^2\theta} \times \frac{1}{1+z} \quad (n=0,1,2,\ldots) \quad (1)$$

where B/B_crit is the magnetic field strength in units of the QM critical field $B_\mathrm{crit} = 4.4 \cdot 10^{13}$ G, θ is the angle between the photon and the magnetic field, $m_\mathrm{e}c^2$ is the electron rest energy and z denotes the gravitational redshift. In our approach to model cyclotron line shapes, we use a revised version of a Monte Carlo code developed by Araya et al. [5, 6] including relativistic scattering cross sections and photon spawning. Physical conditions are determined by the choice of magnetic field strength B, plasma geometry, electron parallel temperature T_e, optical depth τ, a relativistic Maxwellian e^- momentum distribution and an isotropic angular distribution of the injected Monte Carlo photons. Calculations are valid for the low-density / high-field ($B < B_\mathrm{crit}$) regime of internally irradiated plasmas. Our model is not restricted to any a priori form of continuum radiation.

2. ACCRETION GEOMETRY AND OPTICAL DEPTH

Two extreme cases of plasma geometries in the accretion mound are considered: a cylinder ('cy') of infinite length representing the 'fan beam' scenario (Fig. 2, left) and a slab ('sl') of infinite extension corresponding to the 'pencil beam' radiation form (Fig. 2, right). The plasma is internally irradiated: Continuum source photons are inserted at the cylinder axis or slab mid-plane and then reprocessed in the plasma where the lines form. The B-field is assumed to be parallel to the cylinder axis and perpendicular to the slab plane. The formation of cyclotron lines with increasing optical depth τ for cylinder and slab geometry is shown in Fig. 1.

With increasing optical depth, for both geometries the lines become more pronounced and assume a more complex shape. Furthermore, a significant variation of the line profiles with the angle θ of the escaping photons

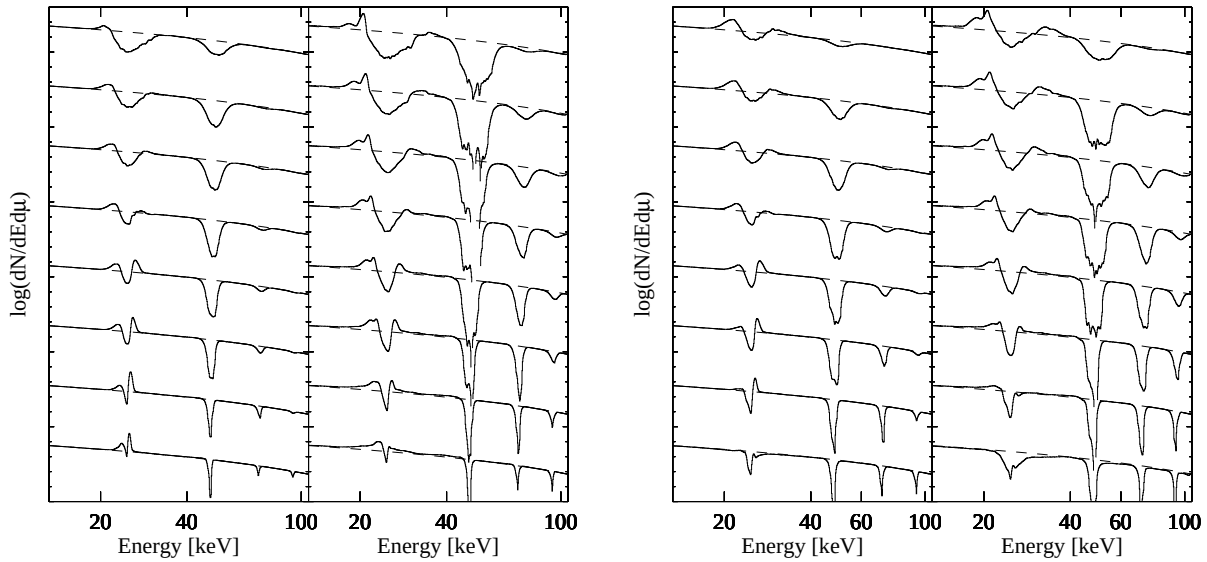

Figure 1. Optical depth progression and variation of the line profiles with the angle θ of the escaping photons. Cyclotron line spectra are shown for both cylinder geometry (left box) and slab geometry (right box). For each geometry, results for two values of τ ($\tau = 3 \times 10^{-4}$ (left) and $\tau = 3 \times 10^{-3}$ (right)) and for eight angular bins $\mu = cos\theta \in (0.000, 0.125)$, $[0.125, 0.250)$, $[0.250, 0.375)$, $[0.375, 0.500)$, $[0.500, 0.675)$, $[0.675, 0.750)$, $[0.750, 0.875)$, $[0.875, 1.000)$, where μ increases from bottom to top, are depicted. $B/B_{\rm crit} = 0.05$ and $kT_{\rm e} = 3.5$ keV were held fixed.

with respect to the magnetic field direction is seen. For smaller θ (increasing $\mu = \cos\theta$) the lines become broader and the second harmonic is shallower. Eight angular bins are depicted for illustration (Fig. 1). The magnetic field strength $B/B_{crit} = 0.05$ and the parallel electron temperature $kT_{\rm e} = 3.5$ keV were held fixed.

2.1. Continuum shape and photon spawning

At present, only phenomenological models are used to explain the continuum of accreting neutron star spectra [8, 9, 10]. Only recently, some theoretical approaches to derive the continuum have emerged [11]. From our cyclotron line simulations, we predict the influence of the assumed continuum shape onto the line profiles (Fig. 3, left) which is governed by the effect of photon spawning (Fig. 3, right).

Photon spawning occurs when an electron, which has been excited by an incident high-energy photon to a higher Landau level n, decays in various steps, generating secondary photons of energies $E_{m<n}$. The right panel of Fig. 3 shows the change of the line profiles for a flat input continuum spectrum, when allowing scattering processes off electrons only at the fundamental energy E_0 (bottom solid line / upper dotted lines) or for up to three harmonics (upper solid lines). In the former case, a single absorption line forms. The more harmonic scatterings are allowed for, the more lines form, while the fundamental and lower harmonics become shallower with growing emission wings. The line shapes thus change with

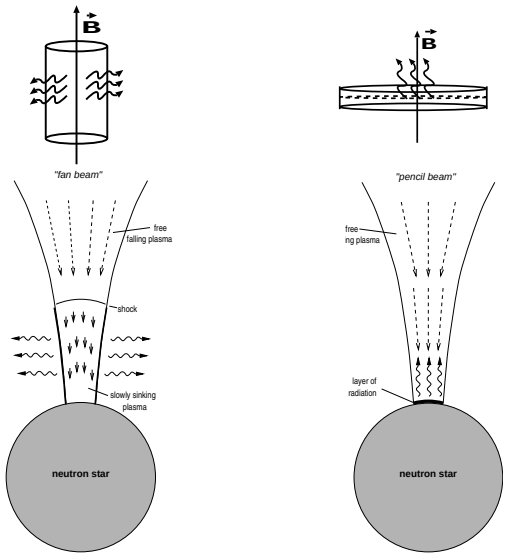

Figure 2. Accretion column geometries. Left: fan beam scenario: For high mass accretion rates [7], a collisionless shock forms and the upscattered high energy photons escape in a wide spread 'fan' beam perpendicular to the B-field. The corresponding simplified geometry is an infinitely long cylinder with photons emerging from its mid-axis. Right: pencil beam scenario: For low mass accretion rates, no shock front forms and the photons may escape in form of a sharp 'pencil' beam along the accretion column. This corresponds to the extreme case of an infinitely extended slab geometry.

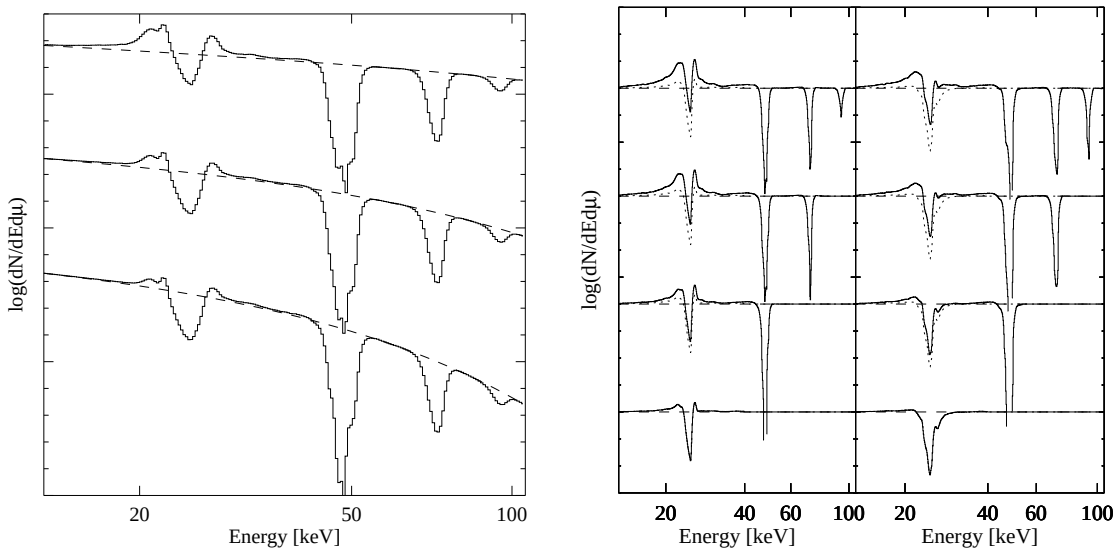

Figure 3. Variation of the line profiles with the continuum shape due to photon spawning. Left: Line profiles for different continuum shapes (continua are of XSPECs `cutoffpl` *form for cutoff energies* $E_{cut} = 10, 20, 100$ *keV from bottom to top.* $B/B_{crit} = 0.05$*,* $kT_e = 3.5$ *keV,* $\tau = 3 \times 10^{-3}$*,* $\mu \in [0.375, 0.5)$*, cy). Right: Effect of photon spawning for up to three harmonics (bottom to top). Line profiles are shown for a flat input continuum spectrum when taking into account scattering processes of electrons with only one times or up to three times the fundamental Landau energy. The shape of the fundamental line for the case that no photon spawning is permitted in the model is overplotted as a dashed line in all plots. Further parameters are chosen as* $B/B_{\rm crit} = 0.05$*,* $kT_{\rm e} = 3.5$ *keV,* $\tau = 3 \times 10^{-3}$*,* $\mu \in [0.125, 0.25)$*, cy/sl.*

the spectral hardness of the incident continuum, where harder spectra exhibit more emission features near shallower lines. Line profiles are shown for a continuum spectrum of the form of a power law with a high-energy exponential cutoff $f(E) = const. \times E^{-\alpha} \times \exp(-E/\beta)$ (*XSPECs* `cutoffpl`) and for different cutoff energies.

3. FITTING V0332+53 DATA

We have created a local *XSPEC* model, `cyclomc`, to allow the direct comparison of observational data with the Monte Carlo simulations. The model interpolates the Monte Carlo results from a previously calculated parameter grid of $B/B_{crit} \in [0.04, 0.1]$, $kT_e \in [2.5, 3.5]$ keV and $\mu = \cos\theta \in (0, 1)$. *INTEGRAL* data of the January 2005 outburst of V0332+53 was chosen for a comparison of this preliminary model to real source data. Modeling the time-averaged spectrum [4] shows that we are able to model the fundamental line shape well. We used an exponentially cutoff power law to model the continuum (Fig. 4, top) and, after convolving it with `cyclomc`, we smeared out the CRSF profiles by applying a `gsmooth` component with constant 3 keV broadening. The latter measure was taken as the Doppler broadening included in our *XSPEC* model is small due to the limited preliminary parameter grid to electron temperatures of only up to 3.5 keV, while from observational studies [12] and from theoretical arguments [13] one expects higher temperatures of the order $kT_e > E_0/4 \sim 6$ keV for V0332+53. The best fit (Fig. 4, bottom) was obtained for cylinder geometry, revealing a magnetic field strength of $B = 2.95 \times 10^{12}$ G, a viewing angle of $\mu = 0.76$ and the plasma electron temperature of $kT_{\rm e} = 3.4$ keV. This serves as a proof of concept that we can physically model observational data, although the fit is not yet ideal.

4. SUMMARY

From Monte Carlo simulations, we have studied the influence of plasma geometry, viewing angle, optical depth and continuum spectral form onto the shape of the cyclotron line. Focusing on the complex shape of the fundamental line, we demonstrate significant variations with photon angle and continuum form. Fitting cyclotron lines with our new local *XSPEC* model `cyclomc` indicates that we can qualitatively explain cyclotron resonance scattering features in real observed source data. Better fit quality should be obtained once our calculations are finished on a bigger grid, and considering phase-resolved spectra. This work is ongoing, aiming at further generalizations of the model to include different angular distributions and non-constant magnetic fields.

REFERENCES

[1] W.A. Heindl et al. CP714, *X-Ray Timing 2003: Rossi and beyond: 323-330*, 2004.

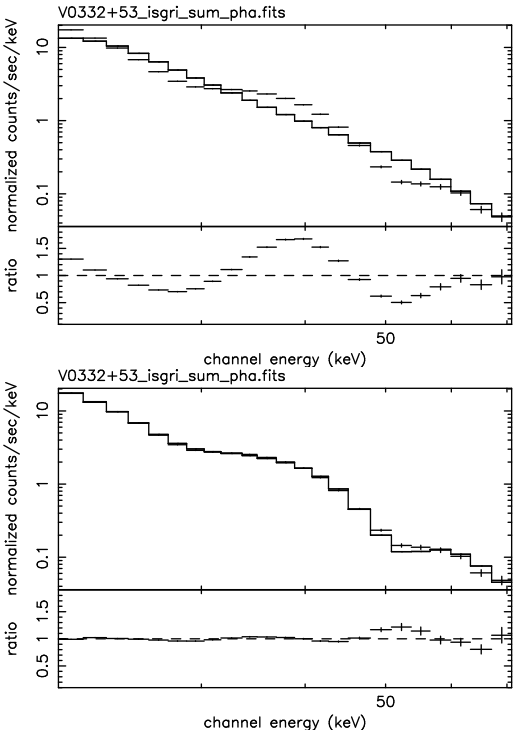

Figure 4. XSPEC fitting of the time-averaged IBIS spectrum from data of the 2005 INTEGRAL observations of the outburst of V0332+53. Left: continuum model: highecut (powerlaw). Right: continuum and lines: highecut (powerlaw)×cyclomc×gsmooth.

[2] A. Santangelo et al. *Bulletin of the American Astronomical Society, Vol.32:1230*, 2000.

[3] K. Pottschmidt et al.*ApJ 634: 97-100*, 2005.

[4] I. Kreykenbohm et al. *A&A 433: L45-48*, 2005.

[5] R. Araya & A. Harding, *ApJ 517: 334-354*, 1999.

[6] R. Araya & A. Harding, *ApJ 544: 1076-1080*, 2000.

[7] M.M. Basko and R.A. Sunyaev, *Mon. Not. R. Astron. Soc. 175: 395-417*,1976.

[8] N.E. White et al. *ApJ 270: 711*, 1983.

[9] Y. Tanaka, *Radiation Hydrodynamics in Stars and Compact Objects: 198*, IAU Coll. No.89 (Springer Verlag), 1986.

[10] T. Mihara, PhD Thesis, RIKEN, Tokyo, 1995.

[11] P. Becker & M. Wolff, *ApJ 630: 465-488*, 2005.

[12] W. Coburn et al. *ApJ 580: 394-412*, 2002.

[13] D. Lamb & J. Wang & I. Wasserman, *ApJ 363: 670-693*, 1990.